







Local burn wound environment versus systemic response: Comparison of proteins and metabolites

Tuo Zang PhD¹  | Kiana Heath BMedLabSci¹ | Joseph Etican BSc¹ |
 Lan Chen PhD² | Donna Langley BSc¹ | Andrew J. A. Holland PhD³  |
 Lisa Martin PhD⁴ | Mark Fear PhD⁴  | Tony J. Parker PhD⁵  |
 Roy Kimble DMed⁶ | Fiona Wood FRACS^{4,7}  | Leila Cuttle PhD¹ 

¹Queensland University of Technology (QUT), School of Biomedical Sciences, Faculty of Health, Centre for Children's Health Research, South Brisbane, Queensland, Australia

²Queensland University of Technology (QUT), Central Analytical Research Facility, Brisbane, Queensland, Australia

³The Children's Hospital at Westmead Burns Unit, Kids Research Institute, Department of Paediatrics and Child Health, Sydney Medical School, The University of Sydney, Sydney, New South Wales, Australia

⁴Burn Injury Research Unit, School of Biomedical Sciences, The University of Western Australia, Perth, Western Australia, Australia

⁵Queensland University of Technology (QUT), School of Biomedical Sciences, Faculty of Health, Kelvin Grove, Queensland, Australia

⁶Children's Health Queensland, Queensland Children's Hospital, South Brisbane, Queensland, Australia

⁷Burns Service of Western Australia, Perth Children's Hospital and Fiona Stanley Hospital, Perth, Western Australia, Australia

Correspondence

Tuo Zang, Queensland University of Technology, Centre for Children's Health Research, 62 Graham St, South Brisbane, QLD, Australia.

Email: t.zang@qut.edu.au

Funding information

National Health and Medical Research Council, Grant/Award Number: APP#1160492

Abstract

In this study, paired blood plasma (BP) and blister fluid (BF) samples from five paediatric burn patients were analysed using mass spectrometry to compare their protein and metabolite composition. The relative quantification of proteins was achieved through a label-free data independent acquisition mode. The relative quantification of metabolites was achieved using a Shimadzu Smart Metabolite Database gas chromatography mass spectrometry (GCMS) targeted assay. In total, 562 proteins and 141 individual metabolites were identified in the samples. There was 81% similarity in the proteins present in the BP and BF, with 50 and 54 unique proteins found in each sample type respectively. BF contained keratinocyte proliferation-related proteins and blood plasma contained abundant blood clotting proteins and apolipoproteins. BF contained more carbohydrates and less alpha-hydroxy acid metabolites than the BP. In this study, there were unique proteins and metabolites in BF and BP which were reflective of the local wound environment and systemic environments respectively. The results from this study

Abbreviations: BF, blister fluid; BP, blood plasma; CHW, The Children's Hospital at Westmead; DDA, data dependent acquisition; DIA, data independent acquisitions; DTT, dithiothreitol; FASP, filter aided sample preparation; GC, gas chromatography; LC, liquid chromatography; MRM, multiple reaction monitoring; MS, mass spectrometry; PCA, principal component analysis; PCV, pooled coefficient of variation; PEV, pooled estimate of variance; PLS-DA, partial least squares discriminant analysis; PMAD, pooled median absolute deviation; QCH, Queensland Children's Hospital; SWATH, sequential window acquisition of all theoretical fragment ion spectra; TBSA, total body surface area; TEAB, triethylammonium bicarbonate; TOF, time-of-flight; VSN, variance stabilisation normalisation; WF, wound fluid.

This is an open access article under the terms of the [Creative Commons Attribution-NonCommercial-NoDerivs](https://creativecommons.org/licenses/by-nc-nd/4.0/) License, which permits use and distribution in any medium, provided the original work is properly cited, the use is non-commercial and no modifications or adaptations are made.

© 2022 The Authors. *Wound Repair and Regeneration* published by Wiley Periodicals LLC on behalf of The Wound Healing Society.

demonstrate that the biomolecule content of BF is mostly the same as blood, but it also contains information specific to the local wound environment.

KEYWORDS

burns, child, metabolite, paediatric, plasma, protein, wound fluid

1 | INTRODUCTION

Burns in children are often relatively minor, but have high morbidity related to scarring and psychological trauma.¹ Biomarkers which can accurately predict which patients are more likely to have adverse healing outcomes could be used to provide earlier, more effective treatment. While mass spectrometry (MS) based proteomic and metabolomic techniques have matured over the past two decades, only a few studies have utilised these techniques to study burn injuries.^{2–8} Label-free MS techniques, based on the biophysical properties of molecules, have enabled the large-scale and robust quantification of patient samples.^{7,9,10} In recent years, a variety of fluid sample types have been used for burn injury analysis and biomarker identification, such as blood (plasma or serum),^{7,8} BF,^{2–5} wound fluid (WF)⁵ and saliva.¹¹ BF and WF have attracted more interest recently as a valuable sample source, as they are thought to reflect both the systemic and local microenvironmental pathological changes as part of the response to injury.^{6,12} BF and WF are produced through the permeation and perfusion of blood to the wound site, and are thought to be similar to plasma in composition. However, present unknowns include the extent of their similarity to plasma, their role in burn injury pathophysiology and wound healing and whether the presence of BF and WF can benefit wound healing or if they are a byproduct of wound healing. Some studies have compared suction BF to plasma from healthy people to investigate drug pharmacokinetics,^{12–16} but there has been no comparison of burn BF with plasma from burn patients. To investigate these differences, we compared blood and BF samples from the burn patients using proteomic and metabolomic analyses.

2 | METHODS AND MATERIALS

2.1 | ETHICAL APPROVAL

Institutional ethics approval for this study was obtained for the collection of samples from Queensland Children's Hospital (QCH) and the Children's Hospital at Westmead (CHW) (HREC/19/QCHQ/48683, SSA/19/QCHQ/48683, RGS0000003284, 2019/STE16483) and from the QUT Human Ethics Committee (#2021000233).

2.2 | Patient recruitment and sample collection

Paediatric burn patients who had burn blisters on presentation and required treatment procedures under sedation in the operating

theatre were recruited from two hospital sites; QCH and CHW. The children and their parents/guardians provided informed consent when recruited into the study. BF was collected during blister deroofing, as part of routine acute wound cleaning procedures. Blood was collected when the participant was receiving routine wound care treatment under a general anaesthetic, to isolate blood plasma (BP). Cellular debris was removed from the BF samples by centrifugation at 855g for 3 min and the supernatant was stored in aliquots at -80°C . The blood was collected in heparinised tubes, centrifuged at 400g for 10 min and the supernatant was stored in aliquots at -80°C . Patient demographics (age, gender), burn wound characteristics (total body surface area [TBSA], depth, mechanism, first aid treatment), treatments and healing outcomes (days until wound re-epithelialisation, referral to scar management, requirement for grafting) were recorded. The burn wound characteristics were determined by the consultant surgeon in conjunction with the clinical treating team.

2.3 | Sample preparation for proteomics

Individual BF and BP samples were processed using the standard FASP digestion method described previously.⁵ In brief, 200 μl of urea buffer (8 M urea [Sigma, #U5128] in 0.1 M Tris/HCl, pH 8.5, 0.025 M DTT) was added to an aliquot of 200 μg total protein from each sample and transferred into Microcon YM-10, 10 kDa NMWCO centrifugal filter devices (Merck Millipore, Bayswater, Victoria, Australia). The centrifugal filter devices were centrifuged at 14,000g for 10 min. The rinse buffer was then replaced by 0.05 M TEAB (Sigma-Aldrich, Castle Hill, New South Wales, Australia) and trypsin was added in a ratio with total protein of 1:100 (w/w) for 18 h at 37°C . The digested peptides were desalted and concentrated using custom-made Stage-Tips prepared as described elsewhere.¹⁷ Indexed Retention Time (iRT) peptides (Biognosys, Switzerland) were spiked into each individual sample at 1:100 ratio.

2.4 | Sample preparation for metabolomics

The metabolites were extracted based on a previously reported plasma and serum extraction method.¹⁸ Individual BF and BP samples were thawed on ice for 60 min. An aliquot of 10 μl sample was combined with 50 μl of ice-cold methanol, vortexed for 15 s and incubated on ice for 15 min to precipitate proteins. The precipitated protein was centrifuged at 4°C and 15,800g for 15 min. The supernatant was transferred directly into a GCMS vial and dried down in a centrifugal vacuum evaporator for 4 h at 30°C .

2.5 | Proteomics analysis

Both data dependent and independent acquisitions (DDA and DIA, respectively) were performed in an Eksigent 400 nanoLC system tandem A Triple TOF 6600 mass spectrometer (SCIEX, Mt Waverley, Victoria, Australia). Samples were first loaded into Trajan ProteCol trap column (120 Å, 3 µm, 10 mm × 300 µm) and flushed for 3 min at 10 µl/min (0.1% formic acid) prior to elution onto the analytical column. The peptides were eluted from a C18 nano-LC resolving column (Eksigent ChromXP C18 3 µm 120 Å [3C18-CL-120], 3 µm, 120 Å, 0.3 × 150 mm) with an 87 min gradient at a flow rate of 5 µl/min. The gradient starts with a 68 min linear gradient of Buffer B (0.1% formic acid [v/v] in acetonitrile) from 3% to 25%, followed by a 5 min linear gradient of 25%–35% mobile phase B. Then the column was flushed with 80% mobile phase B for 5 min and re-equilibrated with 97% Buffer A (0.1% formic acid) for 8 min before the next injection.

The MS parameters for DDA and DIA (sequential window acquisition of all theoretical mass spectra [SWATH]) were set as below: ion spray voltage floating 5500 V, curtain gas 30, interface heater temperature + 100°C, ion source gas 1 and gas 2 both set at 30, and de-clustering potential 80 V. For DDA parameters, 0.25 s MS survey scan in the mass range m/z 400–1250 were followed by 30 MS/MS scans in the mass range of 100–1500 Da (0.05 s per each scan). SWATH variable windows were calculated through *SWATH Variable Window Assay Calculator Version 1.1* [SCIEX, March 9, 2020], with a set of 100 overlapping windows over the range m/z 389.5–1250.5 (1 m/z for the window overlap), based on precursor m/z frequencies in DDA run. In this method, time-of-flight (TOF) MS scans were collected over a range of m/z 350–1500 for 0.05 s, then the 100 predefined m/z ranges (SWATH windows) were sequentially subjected for TOF MS/MS scans over the range of m/z 100–1800 and 0.05 s per window resulting in the total duty cycle of 3.1 s.

2.6 | GCMS targeted metabolomics analysis

The dried samples were loaded onto the GCMS (Shimadzu TQ 8050 NX, Kyoto, Japan) through an online AOC 6000 plus auto-sampler (Shimadzu) for chemical derivatisation and sample injection. The derivatisation was achieved through addition of 25 µl of 30 mg/ml methoxyamine hydrochloride in pyridine and incubation at 37°C for 120 min with vortexing at 700 rpm. An aliquot of 25 µl of *N,O*-Bis(trimethylsilyl)trifluoroacetamide (BSTFA) was also added, with further incubation at 37°C for 60 min with vortexing at 700 rpm. Derivatised sample was then incubate at room temperature for 1 h. One microliter of the derivatised samples was injected onto the GCMS-TQ8050 NX system and analysed in MRM mode using the Shimadzu Smart Metabolite Database containing 521 MRM metabolite targets.^{19,20}

Blank samples were run six times at the beginning and the end of the batch. Quality control (QC) samples, which contained glyoxylic acid (Sigma, # 10601-10G), pyruvic acid (Sigma, # 107360-25G), alanine (Sigma, # AAS18-5mL), glycine (Sigma, # AAS18-5mL), oxalic acid (Sigma, # 73139-100mL), valine (Sigma, # AAS18-5mL), leucine

(Sigma, # AAS18-5mL), isoleucine (Sigma, # AAS18-5mL), proline (Sigma, # AAS18-5mL), succinic acid (Sigma, # 43057-100mL), fumaric acid (Sigma, # 47910-5G), Serine (Sigma, # AAS18-5mL), threonine (Sigma, # AAS18-5mL), oxalacetic acid (Sigma, # O4126-5G), malic acid (Sigma, # 240176-50G), Aspartic acid (Sigma, # AAS18-5mL), methionine (Sigma, # AAS18-5mL), 2-Ketoglutaric acid (Sigma, # 75890-25G), ornithine (Sigma, # 57197-100MG), glutamic acid (Sigma, # AAS18-5mL), phenylalanine (Sigma, # AAS18-5mL), xylose (Sigma, Monosaccharides Kit, # 47267), arabinose (Sigma, # 47267), asparagine (Sigma, #A4159-25G), rhamnose (Sigma, # R3875-5G), aconitic acid (Sigma, # A3412-1G), glutamine (Sigma, # G8540-25G), Fucose (Sigma, # F2252-5G and F8150-5G), citric acid (Sigma, # 251275-5G), arginine (Sigma, # AAS18-5mL), fructose (Sigma, Monosaccharides Kit, # 47267), mannose (Sigma, Monosaccharides Kit, # 47267), galactose (Sigma, Monosaccharides Kit, # 47267), glucose (Sigma, Monosaccharides Kit, # 47267), lysine (Sigma, # AAS18-5mL), histidine (Sigma, # AAS18-5mL), tyrosine (Sigma, # AAS18-5mL), inositol (Sigma, # 15125-50G and 18132-5MG), tryptophan (Sigma, # T0254-5G), fructose 6-phosphate (Sigma, # F3627-100MG), glucose 6-phosphate (Sigma, # G7250-500MG), and trehalose (Sigma, # PHR1344-500MG) (carbohydrates 0.1 nmol/µl, phosphates 1 nmol/µl, organic acids 0.5 nmol/µl, and amino acids 1 nmol/µl), were run at the beginning, in the middle and at the end of the batch. The metabolite identification and quantification were completed using LabSolutions Insight software (Shimadzu).

2.7 | Ion library generation and SWATH data extraction

The database was created based on a SwissProt human database (generated on 12 February 2019) with the common Repository of Adventitious Proteins (<https://www.thegpm.org/crap/>) and iRT peptide sequences included.²¹ The peptide ion library was generated from the DDA data of a pooled sample of a small aliquot of each individual sample and previous published DDA data using the cloud toolkit OneOmics (SCIEX)³⁻⁵ with a threshold of 1% Global false discovery rate (FDR) at both protein and peptide level. The modified peptides were excluded, the number of peptides per protein was set to 15, and the number of transitions per peptide was set to 6. The Extraction step employed iRT peptides for RT calibration, a 50 ppm extracted ion chromatogram extraction width, and an 8 min XIC extraction window. The MS proteomics data were deposited to the ProteomeXchange Consortium²² via the PRIDE²³ partner repository with the data set identifier PXD034978.

2.8 | Statistical analysis

The raw SWATH protein abundance data and metabolite abundance data were processed using NormalizerDE²⁴ online tool (<http://130.235.214.136/>) to determine the most appropriate normalisation method.²⁵ Comparison between eight different normalisation

methods (\log^2 , Variance Stabilisation Normalisation [VSN], Global Intensity, median intensity, mean intensity, quantile, cyclic locally estimated scatterplot smoothing and Robust Linear Regression), indicated that VSN would provide the lowest variation based on Pooled Coefficient of Variation (PCV), Pooled Median Absolute Deviation (PMAD) and Pooled Estimate of Variance (PEV) for both datasets (Figure S1), and the data were normalised using this method. Patients who had more than one BF sample collected had the average protein abundances of the two samples collated so that the dataset would not be skewed by overrepresentation of that patient. Normalised data were then exported to MetaboAnalyst 4.0 (<http://www.metaboanalyst.ca/>) to undergo multiple statistical analyses (PCA for dimensionality reduction, PLS-DA for further discrimination between fluid types, Student's *t*-test, and correlation heat maps) and visualisation. The normalised proteomic data had a total of 15 missing abundance values when uploaded to MetaboAnalyst, so these were replaced with values that were one fifth of their group's lowest abundance value for that protein. No data filtering was performed. Volcano plots of non-normalised protein abundance data were generated using RStudio (<https://www.R-project.org/>) and the R package ggplot2 to visualise the relationship between fold change and the *p*-values derived from MetaboAnalyst. Two-fold change and 1.8-fold change were used to capture an appropriate number of proteins and metabolites, respectively. The gene ontology enrichment analysis of the proteomics was performed using Cytoscape²⁶ v3.9.1 (<https://cytoscape.org/>)²⁶ with the BiNGO application (<http://apps.cytoscape.org/apps/bingo>),²⁷ for the unique proteins identified in the BF and plasma samples and the significant proteins (*p* < 0.05) with high fold change (≥ 2) from the volcano plot. In brief, a hypergeometric test and Benjamini and Hochberg FDR correction were used for over-representation analysis and the significance level of the biological process, cellular component, or molecular function was set at 0.05. The pathway enrichment analysis of the proteomics and metabolomics was performed using MetaboAnalyst, Hypergeometric Test was used for enrichment analysis, topology measure was degree centred, and the integration was *p*-value combined at the pathway-level. The box and whisker plots were created with GraphPad Prism v9.3.1 (California), and the *p*-values for these plots were calculated using raw, unnormalized data, which was different from the *p*-values above.

3 | RESULTS

In order to have the most unbiased analysis, we collected BF and BP samples from the same patient. A total of 12 samples from five patients were collected: 5 BP and 7 BF. The patient demographics and burn wound characteristics are shown in Table 1.

To compare the protein composition of BF and BP, a total of 562 proteins were identified in these two types of sample, and 81% (458) of these proteins were common to both the BP and BF (Figure 1A). There were 50 proteins unique to the BP, and 54 proteins unique to the BF (Table S1). A total of 141 metabolites (including some heavy isotopes) were identified in both BF and BP. There

TABLE 1 Demographic table of blister fluid and blood plasma matched sample patients (*n* = 5)

	N	%		
Patients	5			
Sex				
Male	5	100		
Female	0	0		
Depth (by clinical judgement)				
Superficial partial thickness	2	40		
Deep partial thickness	2	40		
Full thickness	1	20		
Mechanism of injury				
Scald	2	40		
Flame	3	60		
Skin grafting				
Yes	1	20		
No	4	80		
	Median	Range		
Age at injury (months)	66	6–137		
Burn total body surface area (%)	6	3–10		
Collection day post-burn	0.6	0.2–0.8		
Days to re-epithelialisation	22	10–46		
	Blister fluid		Blood plasma	
Samples	7 ^a	5		
	Median	Range	Median	Range
Protein concentration (mg/ml)	58.3	48.5–61.4	72.0	46.1–74.2

^aTwo patients had two blisters.

were 34 amino acids, 34 carbohydrates, 20 fatty acids, 5 alpha hydroxy acids, 4 beta hydroxy acids and some other organic compounds. When comparing the total metabolite abundance in each subclass between BF and BP (Figure 1B), most subclasses had similar abundance in the two sample types. The biggest difference was the alpha hydroxy acids, which were 15.4% of all metabolite abundance in BP but only 8.2% in BF. Additionally, the carbohydrates in BF were 6.1% higher than in BP (38.5% vs. 32.4%). It is worth noting that the 20 fatty acids only accounted for about 1% of total metabolite abundance.

To determine whether the proteome and metabolome can differentiate between BF and BP, a PCA analysis of the protein abundance of all samples was applied (Figure 2A) and showed there was a complete separation between the two groups, suggesting very distinct protein compositions of the BF and BP samples. Interestingly, the 50_5 BF and 50_5 BP samples (which were collected from a different hospital site to the remaining samples) were more separated from the rest of the samples. Similar results were observed for the metabolomics PCA of the same samples (Figure 2B), there was only slight overlap around sample 50_5 BF and 50_5 BP.

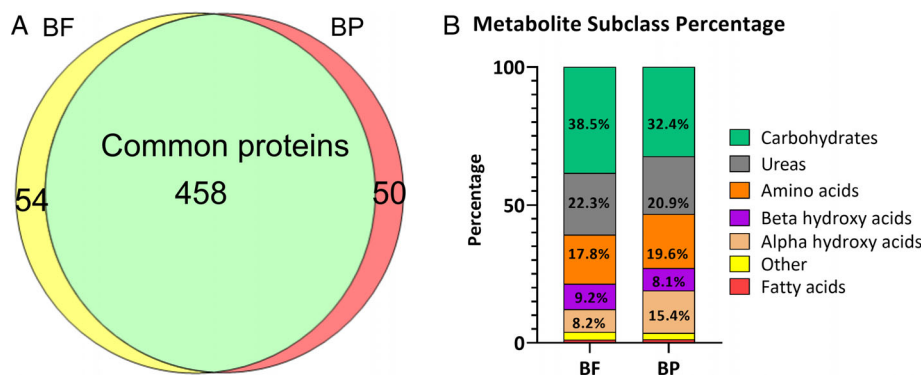


FIGURE 1 Comparison of the proteins and metabolites in BF and BP. (A) Venn diagram of proteins identified in matched BF versus BP samples, $n = 12$. There are 81% common proteins between BF and BP. (B) The fraction (%) of subclasses of metabolites identified in BF and BP samples, based on the abundance of the metabolites, $n = 12$. [Color figure can be viewed at wileyonlinelibrary.com]

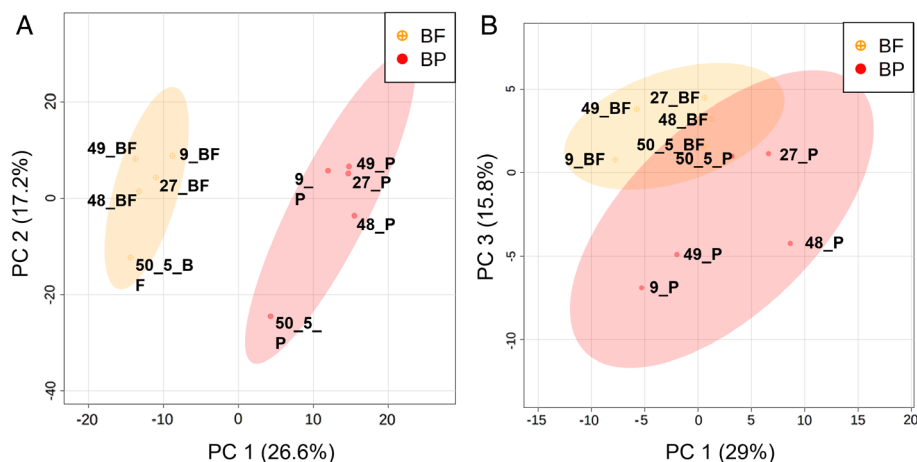


FIGURE 2 BF and BP exhibit distinct protein and metabolite profiles. PCA plots based on the protein and metabolite abundance within each sample. (A) Unsupervised PCA plot based on the VSN normalised protein abundance between BF and BP, $n = 12$. (B) Unsupervised PCA plot based on the VSN normalised metabolite abundance between BF and BP, $n = 12$. [Color figure can be viewed at wileyonlinelibrary.com]

In order to determine what proteins and metabolites have the largest alteration between BF and BP, the scores of variable importance in projection (VIP) from the partial least-squares discriminant analysis (PLS-DA) was utilised and this showed the 15 proteins (Figure 3A) and 15 metabolites (Figure 3B) that most contributed to the differentiation between the BF and the BP matched samples. Notably, histone proteins (H2B Clustered Histone 18 [H2BC18], H2A Clustered Histone 20 [H2AC20], H2A Clustered Histone 18 [H2AC18], H1.3 Linker Histone [H1-3]) are higher in BF samples, and Haemoglobin subunit alpha (HBA1), Haemoglobin subunit beta (HBB), blood clotting-related proteins—Fibrinogen alpha chain (FGA), Fibrinogen beta chain (FGB), Fibrinogen Gamma Chain (FGG), Glycoprotein V Platelet (GP5) are higher in BP (Figure 3A). In the metabolomic analysis, 5-Methoxytryptamine, Cholesterol, Mannitol, Taurine, Taurine-13C2, Lactic acid, Octanoic acid and Trehalose had a higher abundance in BP. However, 2-Ketobutyric acid, Pyruvic acid, Turanose, Glutamic acid, 2-Ketoglutaric acid, Sorbose and Galactose were more abundant in BF (Figure 3B).

To see the proteome and metabolome similarity between samples and the abundance change in each individual sample of top protein and metabolites, a dendrogram clustering and heatmap was used for visualisation (Figure 4). This showed that the samples were clustered into separate groups, with clear distinction between the proteins and metabolites present within the BP and BF samples. The heatmap also showed that there was a distinct separation in the abundance

differences in the samples, as seen by the colour intensity differences. Heat Shock Protein Family B Member 1 (HSPB1), H4 Clustered Histone 1 (H4C1), H2AC20, H2BC18, H2AC18, H1-3, GC Vitamin D Binding Protein (GC), Triosephosphate Isomerase 1 (TPI1), Serine Peptidase Inhibitor Kazal Type 5 (SPINK5), Stratifin (SFN), Histone H2B type 1-M (H2BC14) and YWHAE were decreased (blue) in almost all the BP samples (Figure 4A). Complement C1s (C1S), Apolipoprotein C1 (APOC1), PF4V1, HBA1, HBB, FGG, FGB, FGA, Immunoglobulin J chain (JCHAIN), THBS1, Protein S (PROS1), PPBP and Apolipoprotein L1 (APOL1) were increased in almost every BP sample. The metabolomics results were slightly more variable, however it was still apparent that 4-Hydroxyphenyllactic acid, Fucose, Lactic acid, 5-Methoxytryptamine, Cholesterol, Taurine, Docosahexaenoic acid and Monostearin have a higher abundance in BP, whereas Pyruvic acid, 2-Ketoglutaric acid, Ornithine, Dopamine, Tyrosine, Tyramine, Lysine, Cystine and 2-Ketobutyric acid have a higher abundance in BF (Figure 4B).

To determine the proteins with both large fold change and high significance, volcano plots were utilised. Volcano plot analysis revealed several significant ($p \leq 0.05$) proteins that exhibited greater than twofold difference in abundance between BF and BP samples. The most significant proteins that exhibited a lower abundance in BF were Fibrinogen alpha chain (FGA), Platelet Factor 4 Variant 1 (PF4V1), Fibrinogen beta chain (FGB) and Pro-Platelet Basic Protein (PPBP) ($p < 0.05$) (Figure 5A). Conversely, H2A Clustered Histone 20 (H2AC20), H1.3 Linker Histone (H1-3), H2B Clustered

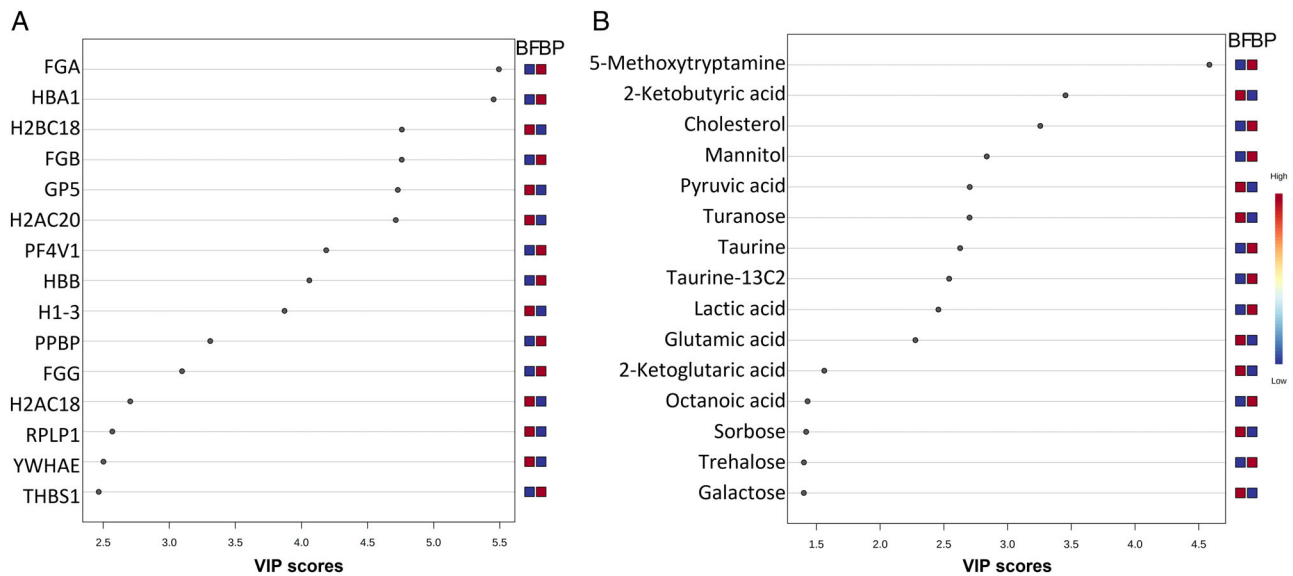


FIGURE 3 The proteins and metabolites which most discriminate between the BF and BP samples in supervised partial least-squares discriminant analysis (PLS-DA). (A) Top 15 proteins with highest variable importance in projection (VIP) scores, fibrinogen alpha chain (FGA), haemoglobin subunit alpha (HBA1), histone H2B type 2-F (H2BC18), fibrinogen beta chain (FGB), platelet glycoprotein V (GP5), histone H2A type 2-C (H2AC20), platelet factor 4 variant (PF4V1), haemoglobin subunit beta (HBB), histone H1.3 (H1-3), platelet basic protein (PPBP), fibrinogen gamma chain (FGG), histone H2A type 2-A (H2AC18), 60S acidic ribosomal protein P1 (RPLP1), 14-3-3 protein epsilon (YWHAE), and thrombospondin-1 (THBS1). (B) Top 15 metabolites with highest VIP scores. [Color figure can be viewed at wileyonlinelibrary.com]

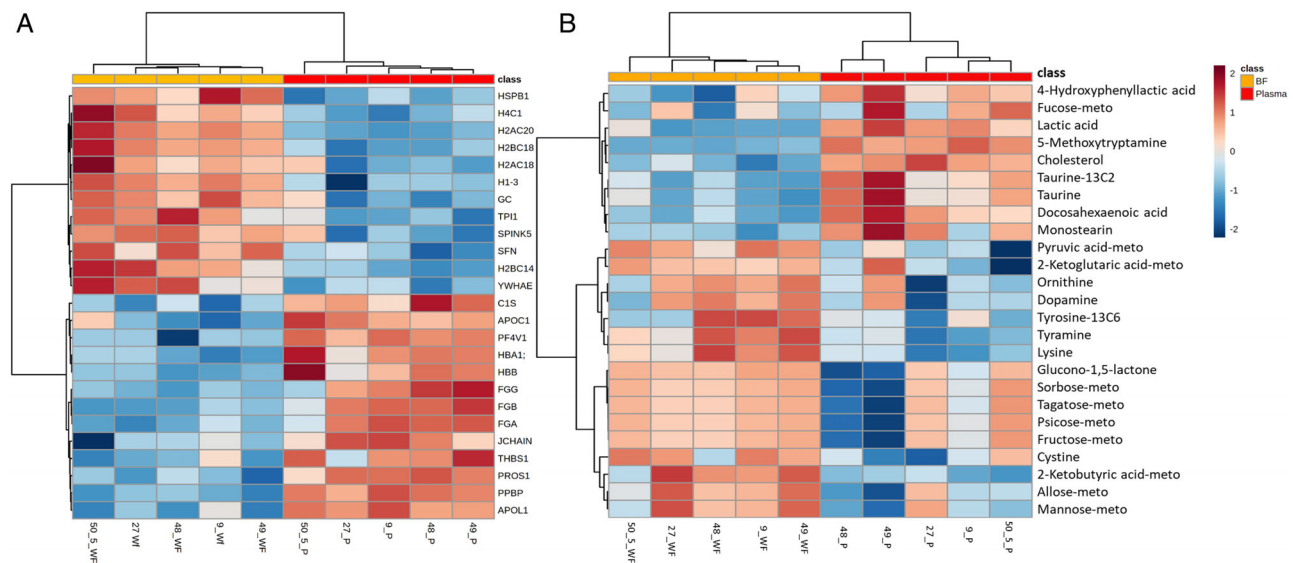


FIGURE 4 Most significant protein and metabolite abundance changes in each individual sample, based on p value. Red in the heatmap indicates higher abundance and blue indicates lower abundance. Yellow in the top bar represents BF samples and red represents BP samples. (A) Top 25 most significant proteins. Heat shock protein beta-1 (HSPB1), histone H4 (H4C1), histone H2A type 2-C (H2AC20), histone H2B type 2-F (H2BC18), histone H2A type 2-A (H2AC18), histone H1.3 (H1-3), vitamin D-binding protein (GC), triosephosphate isomerase (TPI1), serine protease inhibitor Kazal-type 5 (SPINK5), 14-3-3 protein sigma (SFN), histone H2B type 1-M (H2BC14), 14-3-3 protein epsilon (YWHAE), complement C1s subcomponent (C1S), apolipoprotein C-I (APOC1), platelet factor 4 variant (PF4V1), haemoglobin subunit alpha (HBA1), haemoglobin subunit beta (HBB), fibrinogen gamma chain (FGG), fibrinogen beta chain (FGB), fibrinogen alpha chain (FGA), immunoglobulin J chain (JCHAIN), thrombospondin-1 (THBS1), vitamin K-dependent protein S (PROS1), platelet basic protein (PPBP) and apolipoprotein L1 (APOL1). (B) Top 25 most significant metabolites. [Color figure can be viewed at wileyonlinelibrary.com]

Histone 14 (H2BC14) and Tyrosine 3-Monooxygenase/Tryptophan 5-Monooxygenase Activation Protein Epsilon (YWHAE), exhibited a significantly higher abundance in BF ($p < 0.05$) (Figure 5A). Similarly,

some significant metabolites ($p \leq 0.05$) exhibited a fold change greater than $\times 1.8$ between BF and BP (Figure 5B). The abundance of 5-Methoxytryptamine, Lactic acid, Taurine-13C2, Cholesterol, and

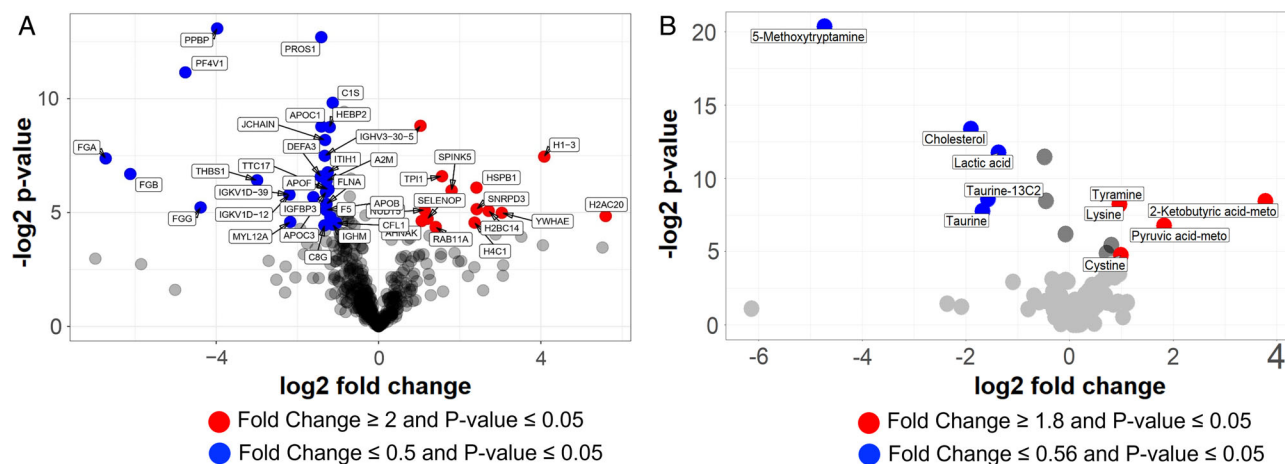


FIGURE 5 Significant proteins and metabolites which also showed large fold change differences in abundance between BF ($n = 5$) and BP ($n = 5$) samples. Red points have higher abundance in BF while blue points have a higher abundance in BP. Grey points are $p > 0.05$. (A) Significant proteins with ≥ 2 -fold change. Heat shock protein beta-1 (HSPB1), histone H4 (H4C1), histone H2A type 2-C (H2AC20), histone H2B type 2-F (H2BC18), histone H2A type 2-A (H2AC18), histone H1.3 (H1-3), vitamin D-binding protein (GC), triosephosphate isomerase (TPI1), serine protease inhibitor Kazal-type 5 (SPINK5), 14-3-3 protein sigma (SFN), histone H2B type 1-M (H2BC14), 14-3-3 protein epsilon (YWHAE), complement C1s subcomponent (C1S), apolipoprotein C-I (APOC1), platelet factor 4 variant (PF4V1), haemoglobin subunit beta (HBB), fibrinogen gamma chain (FGG), fibrinogen alpha chain (FGB), fibrinogen alpha chain J chain (JCHAIN), thrombospondin-1 (THBS1) and vitamin K-dependent protein S (PROS1). (B) Significant metabolites with ≥ 1.8 -fold change. [Color figure can be viewed at wileyonlinelibrary.com]

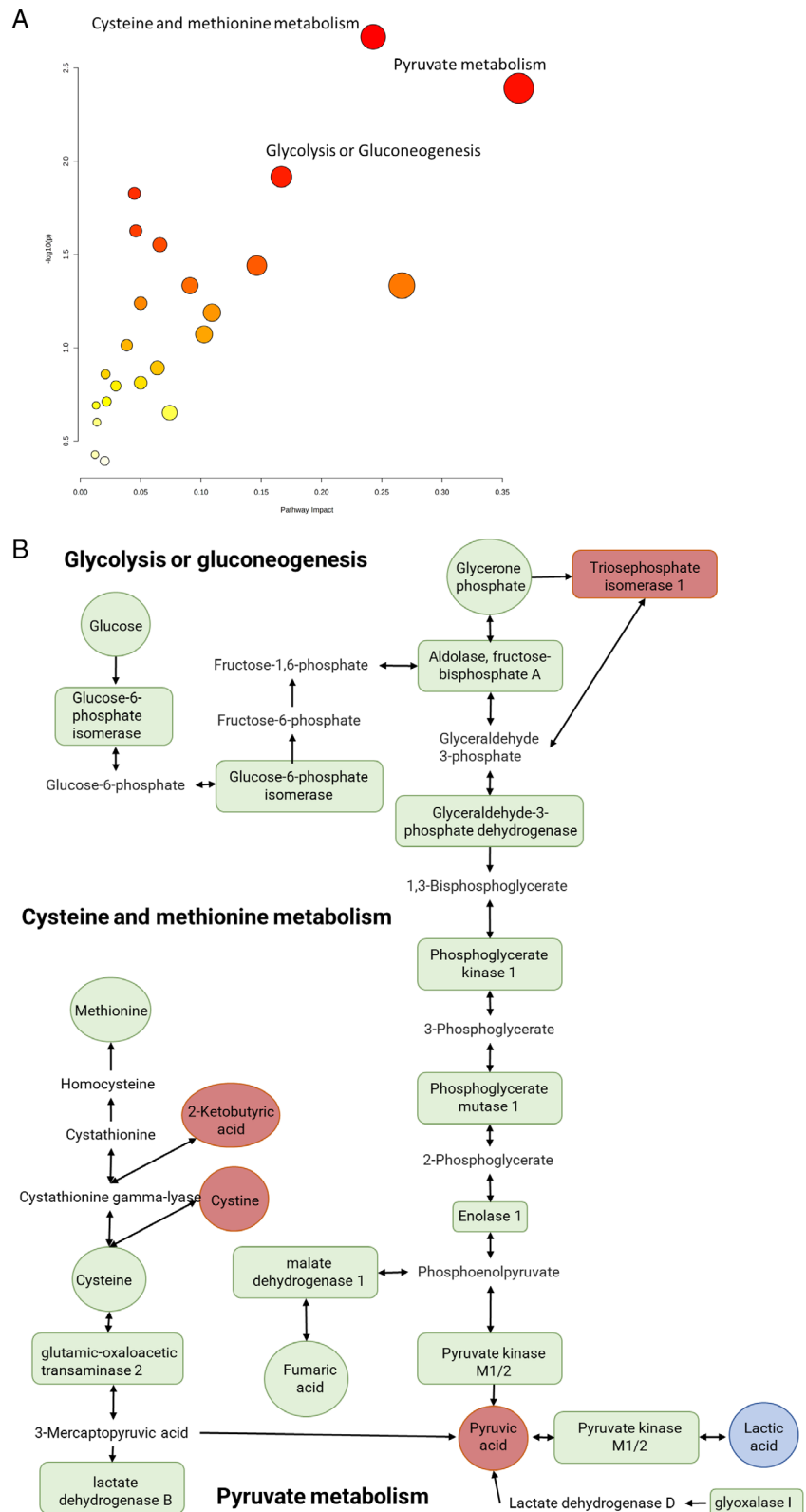
TABLE 2 Gene ontologies overrepresented in the BF and BP proteomes

	Biological process	Cellular component	Molecular function
Blister fluid	Actin filament polymerisation	Extracellular region	
	Protein polymerisation	Extracellular space	
	Epidermis development	Extracellular region part	
	Actin polymerisation or depolymerisation	Membrane-bounded vesicle	
	Ectoderm development	Vesicle	
	Response to organic substance	Desmosome	
	Macromolecular complex subunit organisation	Soluble fraction	
	Disruption by host of symbiont cells	Pigment granule	
	Killing by host of symbiont cells	Melanosome	
	Positive regulation of cell proliferation	Cytoplasmic membrane-bounded vesicle	
Blood plasma	Response to wounding	Platelet alpha granule	Eukaryotic cell surface binding
	Blood coagulation	Vesicle lumen	Cell surface binding
	Coagulation	Extracellular region	Receptor binding
	Haemostasis	Platelet alpha granule lumen	Actin binding
	Lipoprotein particle clearance	Cytoplasmic membrane-bounded vesicle lumen	Cholesterol binding
	Killing of cells of another organism	Cytoplasmic vesicle part	Threonine-type endopeptidase activity
	Very-low-density lipoprotein particle assembly	Stored secretory granule	Threonine-type peptidase activity
	Response to stress	Extracellular space	Sterol binding
	Regulation of body fluid levels	Fibrinogen complex	Lipid binding
	Regulation of Actin polymerisation or depolymerisation	Extracellular region part	Calcium-dependent protein binding

Note: Proteins which were unique to each fluid type or which were significantly different ($p \leq 0.05$) and had higher (≥ 2) or lower (≤ 0.05) fold change in abundance were included in the analysis.

Taurine all were significantly lower in BF compared with BP, whereas 2-Ketobutyric acid, Pyruvic acid, Cystine, Tyramine and Lysine all had a higher abundance in BF compared with BP (Figure 5B).

To investigate the underlying biological processes, molecular functions, and cellular components in each of the sample types, a Gene Ontology enrichment analysis was performed using the unique proteins and over-represented proteins ($p \leq 0.05$ and fold change ≥ 2).



in BF and BP respectively (Table 2). The 10 most significant terms in Biological Process, Cellular Component (CC) and Molecular Function (MF) showed that the BF protein profile represents more local responses including biological processes such as *actin filament polymerisation*, *epidermis development*, *ectoderm development* and *positive regulation of cell proliferation*, which are all related to wound closure and healing. On the other hand, the BP protein profile exhibited more systemic responses to acute burns, including *response to wounding*, *blood coagulation*, *haemostasis*, *response to stress* and *regulation of body fluid levels*. Both BF and BP proteins were overrepresented in

responses against infection, for example *killing by host of symbiont cells* in BF and *killing of cells of another organism* in BP. Although both BF and BP proteins were over-represented in the cellular component for extracellular region, they have different GO annotations. For instance, BF was overrepresented in *pigment granule* and *melanosome*, which are skin related cellular compartments, as well as *membrane-bounded vesicle* and *cytoplasmic membrane-bounded vesicle*. As expected, the BP proteome was overrepresented in *platelet alpha granule* and *fibrinogen complex* as well as *vesicle lumen* and *cytoplasmic membrane-bounded vesicle lumen*. Interestingly, the BF proteome was not

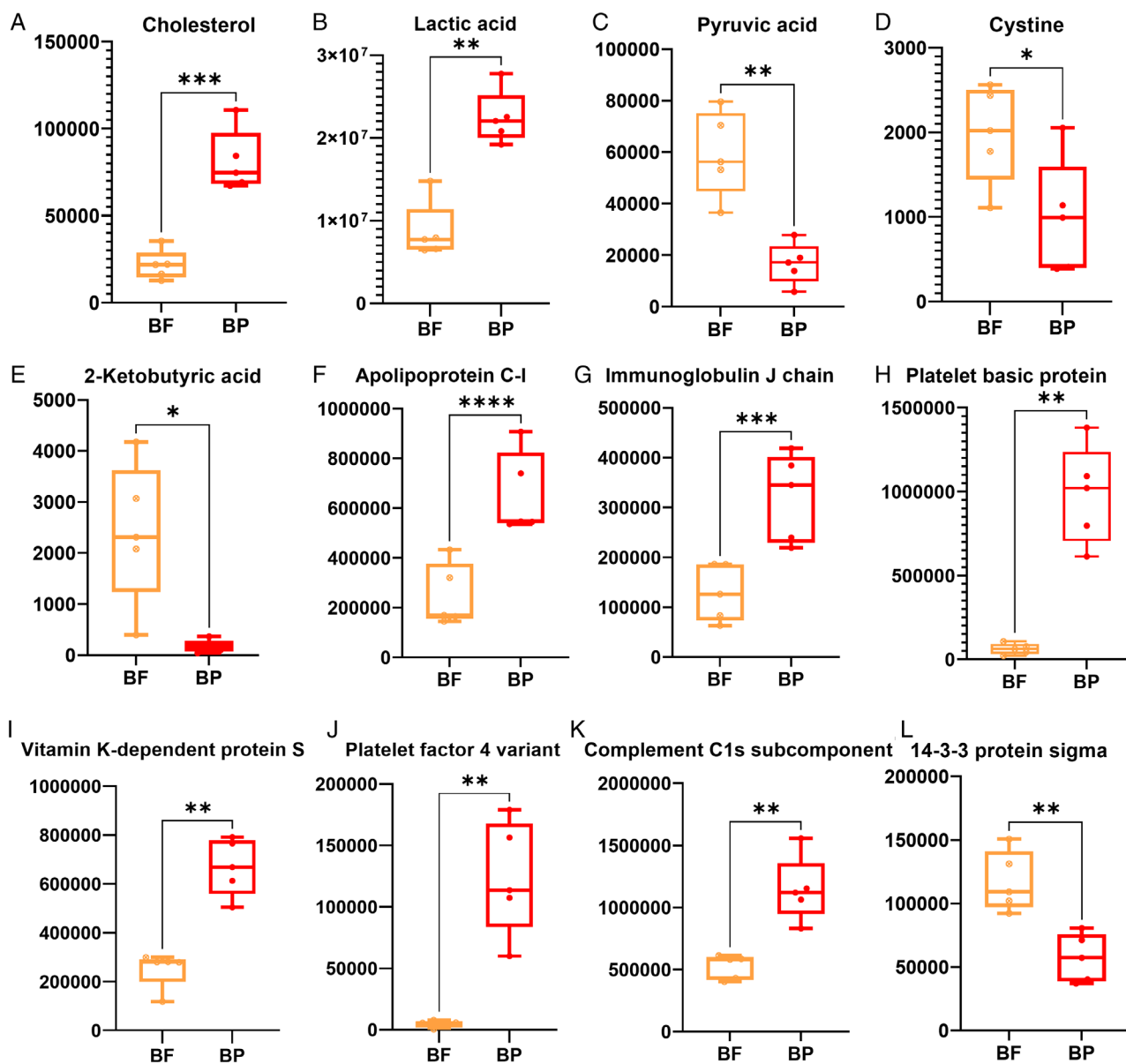


FIGURE 7 Individual protein and metabolite abundance changes between BF and BP. Box-Whisker plots of significant metabolites and proteins, y-axis represents the raw MS intensity. *p*-value is calculated based on raw data, **p* < 0.05, ***p* < 0.01, ****p* < 0.001 and *****p* < 0.0001. Metabolites identified in the enriched pathways (A) cholesterol, (B) lactic acid, (C) pyruvic acid, (D) cystine and (E) 2-ketobutyric acid. Box-Whisker plots of significant proteins with *p*-value < 0.01 and more than 2-fold-change, (F) apolipoprotein C-I, (G) immunoglobulin J chain, (H) platelet basic protein, (I) vitamin K-dependent protein S, (J) platelet factor 4 variant, (K) complement C1s subcomponent and (L) 14-3-3 protein sigma. [Color figure can be viewed at wileyonlinelibrary.com]

significantly overrepresented in any Molecular Functions. However, *cholesterol binding* was overrepresented in the BP proteome, which aligns with the metabolomic results since the cholesterol level was significantly higher in BP than in BF (Figure 5B).

A GO enrichment analysis was also performed using the common proteins in BF and BP (Table S2). The top overrepresented biological processes in common were *acute inflammatory response*, *response to wounding*, *activation of plasma proteins involved in acute inflammatory response*, *inflammatory response*, *complement activation*, *defence response*, *protein maturation by peptide bond cleavage*, *regulation of response to stimulus*, *response to stress and immune response*.

All of the BF samples were collected within 1 day post-burn. During this study, we also had the opportunity to analyse two laser wound fluid (LWF) samples that had been collected from the skin surface during CO₂ ablative laser scar reconstruction treatment of scars, along with matching BP samples also collected at the same time from the same patients. These LWF samples were also essentially acute (laser) burn wound samples but were collected at 5139 and 5812 days post-burn and represented a unique opportunity to examine the role of the local wound environment versus systemic response in a scar. The proteins identified in the LWF samples were very similar to BF, except for only five proteins (Platelet glycoprotein V, Aminopeptidase N, Protein S100-A7, Ganglioside GM2 activator and Immunoglobulin lambda variable 1–36) which were below the limit of detection in some of the BF samples. Likewise, the metabolome subclasses in LWF were the same as BF and BP. However, the quantity of the proteome and metabolome of LWF was very different from both BF and BP (Figure S2). The proportion of amino acids in LWF was much higher than BF, BP and laser scar reconstruction blood plasma (LBP), while alpha and beta hydroxy acids were much lower (Figure S2A). Through the PCA score plot of proteomics, LWF samples were in the middle of BF and BP (Figure S2B), which indicates the LWF protein composition was slightly different to both BF and BP. The metabolomic PCA plot of LWF was quite different from both BF and BP (Figure S2C), which indicates the metabolites present in laser surgery scar wounds were very different from the metabolites in an acute burn injury blister fluid and plasma.

The proteomic and metabolomic data from the blister fluid and blood plasma samples was integrated through pathway enrichment analysis using the 54 significant proteins ($p < 0.05$) and 15 significant metabolites ($p < 0.05$). Cysteine and methionine metabolism; pyruvate metabolism; and glycolysis or gluconeogenesis were the most significantly enriched pathways with a high impact (number of matched hits) (Figure 6A). There were 6 proteins and 4 metabolites identified in the cysteine and methionine metabolism pathway (Figure 6B, left), with cystine, pyruvic acid and 2-ketobutyric acid showing significant abundance change between BP and BF. In the Pyruvate metabolism pathway (Figure 6B, bottom), there were two metabolites which showed significant changes—pyruvic acid and lactic acid, among the seven proteins/metabolites identified in the whole pathway. In the Glycolysis or Gluconeogenesis pathway (Figure 6, top), there were 13 proteins/metabolites identified in the whole pathway, while only triosephosphate isomerase 1, pyruvic acid and lactic acid were significant. In all these three pathways, pyruvic acid and lactic acid were involved.

Through the statistical and pathway enrichment analysis conducted, the abundance levels of a few metabolites and proteins were chosen for further study as they had comparatively high significance levels; large fold change; and were involved in over-represented pathways (for metabolomics only). Cholesterol exhibited the highest significance level and largest fold difference between BF and BP, with lower abundance in BF compared with BP ($p = 0.0002$) (Figure 7A). Lactic acid exhibited a similar abundance difference to cholesterol ($p = 0.0047$) (Figure 7B). Pyruvic acid, cystine and 2-ketobutyric acid all had a higher abundance in BF ($p = 0.0086$; $p = 0.0439$; $p = 0.0174$, respectively) (Figure 7C–E). The proteins Apolipoprotein C-I ($p < 0.0001$) (Figure 7F), Immunoglobulin J chain ($p = 0.0003$) (Figure 7G), Platelet basic protein ($p = 0.0024$) (Figure 7H), Vitamin K-dependent protein S ($p = 0.0014$) (Figure 7I), Platelet factor 4 variant ($p = 0.0047$) (Figure 7J) and Complement C1s subcomponent ($p = 0.0038$) (Figure 7K) were all significantly lower in BF. However, 14-3-3 protein sigma had a higher abundance in BF ($p = 0.0073$) (Figure 7L). These data indicate that although the metabolite and protein composition of BF and BP are mostly the same, the relative abundance of individual proteins and metabolites are significantly different between these two fluids.

4 | DISCUSSION

This study is the first to compare the biochemical composition of matched BF and BP from paediatric burn patients. Through the comparison of 562 proteins and 141 metabolites in each individual sample, we found that BF and BP were mostly similar, although some proteins and metabolites showed significant, large fold abundance changes between the two sample types. The common biological processes between the sample types related to the acute inflammatory response, complement activation and immune/defence response. This indicates that both BF and BP can be used to profile the changes to inflammation and immune response after burn injury, and that blister fluid is a valuable non-invasive biosample in children, to examine levels of these systemic markers without needing to collect blood.

In addition, the unique proteins and metabolites found in BF can provide more information on the local wound healing process, which cannot be obtained from a blood sample. Obvious systemic responses to wounding were observed in the plasma samples, such as *response to wounding*, and *blood coagulation*, and processes which reflect the known fluid loss and dehydration experienced by burn patients,^{28–30} including *haemostasis* and *regulation of body fluid levels*. However, the processes occurring in the BF included *actin filament polymerisation*, *epidermis development*, *ectoderm development* and *positive regulation of cell proliferation*, which indicates that wound healing is already occurring at the wound site and wound healing processes have already been initiated within a few hours after injury. This would suggest BF is a valuable matrix for early clinical prediction of burn wound healing.

In the proteomic analysis, haemoglobin subunit alpha (HBA1) and haemoglobin subunit beta (HBB) were identified in BF. Previous studies by our group and others have also demonstrated an increase in

abundance of these proteins in relation to burn depth, and they can be used as potential biomarkers for burn depth diagnosis in both BF and BP.^{2,31,32} In this study, both HBA1 and HBB had a higher abundance in BP, and this is the first comparison of these proteins between BF and BP from the same patient. This suggested that BP might be used to evaluate HBA1 and HBB for burn depth diagnosis if their abundances are consistent with increasing burn depth. Further investigation of HBA1 and HBB abundance change in BP from patients with different burn depths is required.

Cholesterol exhibited a significant fold change in abundance between BF and BP in this study, with significantly lower cholesterol in the skin exudate, compared with the blood plasma. As BF is a perfusion from BP into the wound, we would expect similar composition of these two body fluids, except for molecules which are consumed/produced at the wound site, or molecules which are deposited into, or transported away in the blood. Cholesterol is mostly stored in the liver, but also in the stratum corneum of the epidermis. It serves to maintain the integrity of cell membranes and it is also a precursor for the formation of steroids, hormones and vitamin D.³³ Previous studies have reported significant decreases of serum cholesterol after severe burn injury,^{34,35} which are associated with poor clinical outcomes, but that is the opposite to reported here. Potentially, after a more minor burn injury, cholesterol is sequestered from the skin and periphery, and this mobilisation of cholesterol enables the quick and successive production of sympathetic nervous system molecules such as epinephrine to aid in the body's defence. Unfortunately, it is difficult to tell whether cholesterol was consumed at the wound site or cholesterol accumulated in the blood as this study did not contain any longitudinal samples, from multiple time points post-burn. Previous studies have also reported increases in serum free-fatty acids post-burn.³⁶ However, there was no significant change in lipids identified in this study. In addition, the identified lipid abundances here were much lower than the amino acids, carbohydrates and other organic acids. The metabolite extraction process used here was a general method for all types of metabolites and GCMS can only measure TMS-derivatised metabolites, which are volatile, semi-volatile and low polar compounds. TMS-derivatisation can reduce the boiling point and polarity of compounds, so for those non-volatile and polar metabolites cannot be derivatised, they cannot be detected in GCMS. In the future, more specific extraction methods could be used for each metabolite subclass and LC-MS based metabolomics could be used to assess non-TMS derivatised metabolites. The use of these techniques and lipidomic assays could improve the identification and quantification of lipids in BF and plasma from burn patients.

Pyruvic acid and lactic acid are both output metabolites from glycolysis, pyruvate is a product of aerobic glycolysis and lactate is a product of anaerobic metabolism, when there is a lack of oxygen. In the hypoxic burn wound environment, lactate is thought to be a mobile energy source, as it can travel in the circulation to the liver, where it is converted to pyruvate through the Cori Cycle, or to other tissues. Lactate and pyruvate are also rapidly interconverted inside cells by lactate dehydrogenase (LDH), and lactate and pyruvate can enter the circulation via cell membrane monocarboxylic

transporters.³⁷ In this study, there was a greater abundance of pyruvate in the tissue, and a greater abundance of lactic acid in the blood. This suggests there is active glycolysis occurring in the tissue, to provide energy for wound healing processes, and pyruvate is produced. As lactic acid is higher in the plasma, this indicates that lactate is being produced from pyruvate and released into the bloodstream,³⁷ to provide an additional energy supply. The lactate shuttle hypothesis describes the generation and distribution of lactate under aerobic and anaerobic conditions, and within and between cells.^{38,39} There is evidence that some lactate within the wound environment can stimulate collagen synthesis, collagen deposition and angiogenesis.^{40–42} However, excess lactate (≥ 20 mmol/L) has been shown to reduce fibroblast cell viability and migration, and has been detected in chronic wound exudate—prompting suggestion that measurement of lactate in wound exudate has potential as a wound diagnostic.⁴³

The comparison of acute wound BF and BP to laser scar wound fluid indicated that ablative laser scar wounds contain more amino acids (and aminopeptidase) and less beta hydroxy acids than acute burns. The molecular differences may be related to the effectiveness of ablative laser in remodelling scarring, and study of additional LWF samples may help to further elucidate these mechanisms. In this study, we were not able to compare acute burn fluid to healthy control tissue fluid, however there have been a few previously reported studies which collected suction blister fluid (SBF) from healthy adults.^{44,45} When we compared the proteins from paediatric burn BF identified in this study with proteins identified in SBF previously, there were 298 proteins in common, with 215 unique proteins in BF and 435 proteins in SBF (Figure S3A). GO enrichment analysis showed that the most unique proteins in burn BF are related to responses to injury, such as *immune system process*, *haemostasis*, *cellular component movement*, *regulation of body fluid levels*, *coagulation and blood coagulation* (Figure S3B). As expected, the unique proteins from SBF did not involve any biological processes related to trauma, although they also reflected the immune response and skin tissue development. These comparisons to other skin fluid samples highlight the unique information that burn blister fluid provides on the burn environment and the healing processes that have been initiated in the burn wound.

The main limitation of this study is that the sample size is small, with matched BF and BP samples collected from only five patients. As not all burns will have blisters on presentation, and BP was only collected when patients were sedated under a general anaesthetic, generally only larger burns or burns in more painful anatomical areas, which also had BF, could be collected. This may have led to bias in the types of proteins and metabolites that were detected. Collection of more samples in the future will bring higher statistical power and enable analyses related to different clinical parameters and outcomes (e.g., re-epithelialization time or scarring). Ideally, the temporal collection of samples over multiple time points after burn injury would provide more information regarding how these metabolic and biological processes change as the burn wound heals. However, serial samples are only possible for BP, as BF is not able to be collected again after the blister is deroofed and the wound is cleaned of devitalised tissue. An alternative option would be to collect wound exudate from

negative pressure therapy⁵ as this would enable multiple collections and monitoring of metabolic changes in inflammatory and healing processes, as the wound heals. In addition, there have been some studies in other areas which indicate that the blood metabolome is associated with age,^{46–48} which means the same person will have different metabolomic profiling at different ages. Therefore, our metabolomic results are limited to paediatric patients and may not be applicable to older burn patients. Moreover, other medical comorbidities will also lead to changes in the blood metabolome, which will also limit the application of our results.

Through this comprehensive comparison of paired proteins and metabolites, we found that the biochemical composition of BF and BP is mostly similar. For clinical diagnostic biomarkers identified in both BF and BP, BF can be an alternative sample source when blood is not available or collection of blood is inappropriate, such as for paediatric patients. However, there are a few proteins and metabolites that exhibit significant (p -value <0.05) abundance change (more than two-fold change). These different biochemical compounds reflect local microenvironmental changes compared with systemic changes after paediatric burn injuries. Therefore, plasma is not the best choice for all diagnostic or pathological analysis. Clinicians and pathologists may need to consider using BF as the sample source when they want to understand the local microenvironment. An early BF sample might also enable clinicians to better predict burn wound healing and the subsequent risk of scarring. This study demonstrates that BF can be a valuable matrix for wound diagnosis and treatment investigations and can provide additional information on the biological processes occurring within the wound. Through a better understanding of the local vs systemic responses, targeted diagnostics for wound status monitoring and locally acting therapies can be developed which can enhance wound healing.

ACKNOWLEDGEMENTS

The authors would like to thank Kira Chamberlain for assisting with patient recruitment, data collection and sample processing and Pawel Sadowski and Raj Gupta at the Central Analytical Research Facility (CARF), Queensland University of Technology (QUT) for assistance with the mass spectrometry. The authors also gratefully acknowledge the paediatric burn patients and their families for providing their samples for analysis. This study was supported by a project grant from the National Health and Medical Research Council #APP1160492. Open access publishing facilitated by Queensland University of Technology, as part of the Wiley - Queensland University of Technology agreement via the Council of Australian University Librarians.

CONFLICT OF INTEREST

The authors have no conflicts of interest to declare.

DATA AVAILABILITY STATEMENT

The raw MS data has been upload to <http://www.proteomexchange.org/> with the dataset identifier PXD034978.

ORCID

Tuo Zang  <https://orcid.org/0000-0002-1280-9638>

Andrew J. A. Holland  <https://orcid.org/0000-0003-3745-8704>

Mark Fear  <https://orcid.org/0000-0003-3163-4666>

Tony J. Parker  <https://orcid.org/0000-0002-5118-524X>

Fiona Wood  <https://orcid.org/0000-0001-5427-6588>

Leila Cuttle  <https://orcid.org/0000-0002-2282-4815>

REFERENCES

- Cuttle L, Fear M, Wood FM, Kimble RM, Holland AJA. Management of non-severe burn wounds in children and adolescents: optimising outcomes through all stages of the patient journey. *Lancet Child Adolesc Health*. 2022;6:269–278.
- Zang T, Cuttle L, Broszczak DA, Broadbent JA, Tanzer C, Parker TJ. Characterization of the blister fluid proteome for pediatric burn classification. *J Proteome Res*. 2018;18:69–85.
- Zang T, Broszczak DA, Cuttle L, Broadbent JA, Tanzer C, Parker TJ. The blister fluid proteome of paediatric burns. *J Proteomics*. 2016;146:122–132.
- Zang T, Broszczak DA, Cuttle L, Broadbent JA, Tanzer C, Parker TJ. Mass spectrometry based data of the blister fluid proteome of paediatric burn patients. *Data Brief*. 2016;8:1099–1110.
- Frear CC, Zang T, Griffin BR, et al. The modulation of the burn wound environment by negative pressure wound therapy: insights from the proteome. *Wound Repair Regen*. 2021;29(2):288–297.
- Zang T, Broszczak DA, Broadbent JA, Cuttle L, Lu H, Parker TJ. The biochemistry of blister fluid from pediatric burn injuries: proteomics and metabolomics aspects. *Expert Rev Proteomics*. 2016;13(1):35–53.
- Finnerty CC, Jeschke MG, Qian WJ, et al. Determination of burn patient outcome by large-scale quantitative discovery proteomics. *Crit Care Med*. 2013;41(6):1421–1434.
- Qian WJ, Petritis BO, Kaushal A, et al. Plasma proteome response to severe burn injury revealed by 18O-labeled "universal" reference-based quantitative proteomics. *J Proteome Res*. 2010;9(9):4779–4789.
- Poulos RC, Hains PG, Shah R, et al. Strategies to enable large-scale proteomics for reproducible research. *Nat Commun*. 2020;11(1):3793.
- Bruderer R, Muntel J, Muller S, et al. Analysis of 1508 plasma samples by capillary-flow data-independent acquisition profiles proteomics of weight loss and maintenance. *Mol Cell Proteomics*. 2019;18(6):1242–1254.
- Carlton M, Voisey J, Jones L, Parker TJ, Punyadeera C, Cuttle L. An exploratory study demonstrating that salivary cytokine profiles are altered in children with small area thermal injury. *J Burn Care Res*. 2021;43:613–624.
- Sjobom U, Christenson K, Hellstrom A, Nilsson AK. Inflammatory markers in suction blister fluid: a comparative study between interstitial fluid and plasma. *Front Immunol*. 2020;11:597632.
- Nilsson AK, Sjobom U, Christenson K, Hellstrom A. Lipid profiling of suction blister fluid: comparison of lipids in interstitial fluid and plasma. *Lipids Health Dis*. 2019;18(1):164.
- Nicolau DP, Sun HK, Seltzer E, Buckwalter M, Dowell JA. Pharmacokinetics of dalbavancin in plasma and skin blister fluid. *J Antimicrob Chemother*. 2007;60(3):681–684.
- Klimowicz A, Nowak A, Bielecka-Grzela S. Plasma and skin blister fluid concentrations of metronidazole and its hydroxy metabolite after oral administration. *Pol J Pharmacol*. 1996;48(1):47–52.
- Niedzwiecki MM, Samant P, Walker DI, et al. Human suction blister fluid composition determined using high-resolution metabolomics. *Anal Chem*. 2018;90(6):3786–3792.
- Rappsilber J, Mann M, Ishihama Y. Protocol for micro-purification, enrichment, pre-fractionation and storage of peptides for proteomics using StageTips. *Nat Protoc*. 2007;2(8):1896–1906.
- Dunn WB, Broadhurst D, Begley P, et al. Procedures for large-scale metabolic profiling of serum and plasma using gas chromatography and liquid chromatography coupled to mass spectrometry. *Nat Protoc*. 2011;6(7):1060–1083.

19. Best SA, De Souza DP, Kersbergen A, et al. Synergy between the KEAP1/NRF2 and PI3K pathways drives non-small-cell lung cancer with an altered immune microenvironment. *Cell Metab.* 2018;27(4):935-943.
20. Bachem A, Makhlof C, Binger KJ, et al. Microbiota-derived short-chain fatty acids promote the memory potential of antigen-activated CD8(+) T cells. *Immunity.* 2019;51(2):285-297 e5.
21. Escher C, Reiter L, MacLean B, et al. Using iRT, a normalized retention time for more targeted measurement of peptides. *Proteomics.* 2012;12(8):1111-1121.
22. Deutsch EW, Csordas A, Sun Z, et al. The ProteomeXchange consortium in 2017: supporting the cultural change in proteomics public data deposition. *Nucleic Acids Res.* 2017;45(D1):D1100-D1106.
23. Vizcaino JA, Csordas A, Del-Toro N, et al. Update of the PRIDE database and its related tools. *Nucleic Acids Res.* 2016;44(D1):D447-D456.
24. Willforss J, Chawade A, Levander F. NormalizerDE: online tool for improved normalization of omics expression data and high-sensitivity differential expression analysis. *J Proteome Res.* 2019;18(2):732-740.
25. Chawade A, Alexandersson E, Levander F. Normalizer: a tool for rapid evaluation of normalization methods for omics data sets. *J Proteome Res.* 2014;13(6):3114-3120.
26. Shannon P, Markiel A, Ozier O, et al. Cytoscape: a software environment for integrated models of biomolecular interaction networks. *Genome Res.* 2003;13(11):2498-2504.
27. Maere S, Heymans K, Kuiper M. BiNGO: a Cytoscape plugin to assess overrepresentation of gene ontology categories in biological networks. *Bioinformatics.* 2005;21(16):3448-3449.
28. Bittner EA, Shank E, Woodson L, Martyn JA. Acute and perioperative care of the burn-injured patient. *Anesthesiology.* 2015;122(2):448-464.
29. Eljaiek R, Heylbroeck C, Dubois MJ. Albumin administration for fluid resuscitation in burn patients: a systematic review and meta-analysis. *Burns.* 2017;43(1):17-24.
30. Smahel J. The problem of dehydration and healing of burn wounds. *Burns.* 1993;19(6):511-512.
31. Wong CH, Song C, Heng KS, et al. Plasma free hemoglobin: a novel diagnostic test for assessment of the depth of burn injury. *Plast Reconstr Surg.* 2006;117(4):1206-1213.
32. Tanzer C, Sampson DL, Broadbent JA, et al. Evaluation of haemoglobin in blister fluid as an indicator of paediatric burn wound depth. *Burns.* 2015;41(5):1114-1121.
33. Schallreuter KU, Hasse S, Rokos H, et al. Cholesterol regulates melanogenesis in human epidermal melanocytes and melanoma cells. *Exp Dermatol.* 2009;18(8):680-688.
34. Gottschlich MM, Jenkins M, Warden GD, et al. Differential effects of three enteral dietary regimens on selected outcome variables in burn patients. *JPEN J Parenter Enteral Nutr.* 1990;14(3):225-236.
35. Vanni HE, Gordon BR, Levine DM, et al. Cholesterol and interleukin-6 concentrations relate to outcomes in burn-injured patients. *J Burn Care Rehabil.* 2003;24(3):133-141.
36. Qi P, Abdullahi A, Stanojic M, Patsouris D, Jeschke MG. Lipidomic analysis enables prediction of clinical outcomes in burn patients. *Sci Rep.* 2016;6:38707.
37. Rabinowitz JD, Enerback S. Lactate: the ugly duckling of energy metabolism. *Nat Metab.* 2020;2(7):566-571.
38. Brooks G. Glycolytic end product and oxidative substrate during sustained exercise in mammals—the “lactate shuttle”. In: Gilles R, ed. *Comparative Physiology and Biochemistry - Current Topics and Trends, Volume A, Respiration - Metabolism - Circulation.* Springer; 1985:208-218.
39. Brooks GA. Intra- and extra-cellular lactate shuttles. *Med Sci Sports Exerc.* 2000;32(4):790-799.
40. Green H, Goldberg B. Collagen and cell protein synthesis by an established mammalian fibroblast line. *Nature.* 1964;204:347-349.
41. Constant JS, Feng JJ, Zabel DD, et al. Lactate elicits vascular endothelial growth factor from macrophages: a possible alternative to hypoxia. *Wound Repair Regen.* 2000;8(5):353-360.
42. Trabold O, Wagner S, Wicke C, et al. Lactate and oxygen constitute a fundamental regulatory mechanism in wound healing. *Wound Repair Regen.* 2003;11(6):504-509.
43. Britland S, Ross-Smith O, Jamil H, Smith AG, Vowden K, Vowden P. The lactate conundrum in wound healing: clinical and experimental findings indicate the requirement for a rapid point-of-care diagnostic. *Biotechnol Prog.* 2012;28(4):917-924.
44. Muller AC, Breitwieser FP, Fischer H, et al. A comparative proteomic study of human skin suction blister fluid from healthy individuals using immunodepletion and iTRAQ labeling. *J Proteome Res.* 2012;11(7):3715-3727.
45. Kool J, Reubsat L, Wesseldijk F, et al. Suction blister fluid as potential body fluid for biomarker proteins. *Proteomics.* 2007;7(20):3638-3650.
46. Wu CS, Muthyala SDV, Klemashevich C, et al. Age-dependent remodeling of gut microbiome and host serum metabolome in mice. *Aging (Albany, NY).* 2021;13(5):6330-6345.
47. Robinson O, Lau CE. Measuring biological age using metabolomics. *Aging (Albany, NY).* 2020;12(22):22352-22353.
48. Shao Y, Li T, Liu Z, et al. Comprehensive metabolic profiling of Parkinson's disease by liquid chromatography-mass spectrometry. *Mol Neurodegener.* 2021;16, (1):4.

SUPPORTING INFORMATION

Additional supporting information can be found online in the Supporting Information section at the end of this article.

How to cite this article: Zang T, Heath K, Etican J, et al. Local burn wound environment versus systemic response: Comparison of proteins and metabolites. *Wound Rep Reg.* 2022;30(5):560-572. doi:10.1111/wrr.13042